Calculation Method and Simulation Study of Optical Efficiency of Fixed-Heaven Mirror Field

Junlan Yue *, #, Wang Guan #, Hongyi Lu #

College of Engineering, Yanbian University, Yanji, China, 133002

* Corresponding Author Email: 18861798204@163.com

#These authors contributed equally.

Abstract. Tower solar thermal power generation is an environmentally friendly new clean energy technology. This paper lays the foundation for constructing a heliostat mirror field with optimal annual average thermal power per unit mirror area by solving the annual average optical efficiency, annual average output thermal power and annual average output thermal power per unit cross-section area for a specific heliostat mirror field. This paper begins with calculating the solar altitude angle and azimuth angle at different times, and derive the normal equation of each heliostat. The specular reflection is studied by taking 100 uniform discrete points on a specular surface and establishing a specular coordinate system, which is used to calculate the ratio of the blocked light to the total light of a single specular surface to indicate the shadow blocking efficiency. The dispersion of light in a single light cone is simulated by establishing a light cone coordinate system for the reflected light, and the ratio of the number of light captured by the collector to the total light is calculated to indicate the truncation efficiency; then the cosine efficiency is calculated by the angle of incidence, and the average annual optical efficiency, average annual output thermal power, and average output thermal power per unit of mirror area are finally derived from the formulas in the relevant literature, and the results are 0.5408, 16.2327 MW, and 0.2584 kW/m^2, respectively.

Keywords: Tower Solar, Heliostat Mirror Field, Optical Efficiency, Output Thermal Power, Coordinate Conversion.

1. Introduction

One of the important measures for China to achieve "carbon peak" and "carbon neutral" is to build a new power system mainly based on new energy sources[1]. Tower solar thermal power generation[2] is a new type of clean energy technology. Tower solar thermal power station consists of a large number of heliostats, absorption towers and collectors, of which heliostats[3] are the basic components for collecting solar energy, reflecting the sunlight to the collectors on the top of the absorption towers, and converting solar energy into heat energy by heating the heat-conducting medium on the collectors, which can be converted into electric energy after heat exchange. An array of many heliostats is called a heliostat field, and a photograph of a heliostat and the circular array arrangement is shown in Figure 1.

Most of the previous studies on heliostats focus on the mirror design and arrangement of heliostats. Based on the angle of heliostat mirrors and the law of solar motion, Liu Jianxing proposed a method to adaptively improve the gravitational constant G(t) in the classical gravitational search algorithm, and after analyzing the composition of the optical efficiency of heliostat mirror fields, the distribution of the optical efficiency, and the related mirror layout methods, he carried out the research on the optimal layout of heliostat mirror fields with the goal of obtaining the highest annual optical efficiency of the mirror fields[4]. Gao Bo et al. proposed a model of the optical efficiency of the fixed-sun mirror field of a photovoltaic power plant based on a mixed-strategy whale optimization algorithm, and obtained the optimal layout scheme[5]. Ding Qi et al. used the projection method of heliostat contour to the ground plane to calculate the shadow and occlusion loss of heliostat mirrors, and introduced a correction factor, which resulted in a method of evaluating the total effective mirror area of heliostat field[6]. However, there are few studies and considerations of the light conduction process in the mirror surface to calculate the efficiency of the heliostat mirror field. In this paper, based on the light cone coordinate system, mirror field coordinate system and mirror coordinate system, and based on the Monte Carlo simulation to simulate the light conduction process in the mirror surface, a suitable mathematical model is constructed, and selected cases for the simulation calculation.

a. Heliostats

b. Circular array of heliostats

Figure 1 Demonstration of heliostat

2. Performance evaluation of fixed-sun mirror field configurations

2.1. Preparation of the model

2.1.1 Relationship between fixed-heaven mirror fields, mirrors, and light

In this paper, three coordinate systems, mirror field coordinate system, mirror coordinate system and light cone coordinate system, are used to describe the spatial relationship among mirror field, mirror and light.

1） Create mirror field coordinate system

Take the center of the circular heliostat mirror field area as the origin, the east direction as the x-axis positive direction, the north direction as the y-axis positive direction, and perpendicular to the ground upward as the z-axis positive direction to establish the mirror field coordinate system.

2） Establishment of the mirror coordinate system

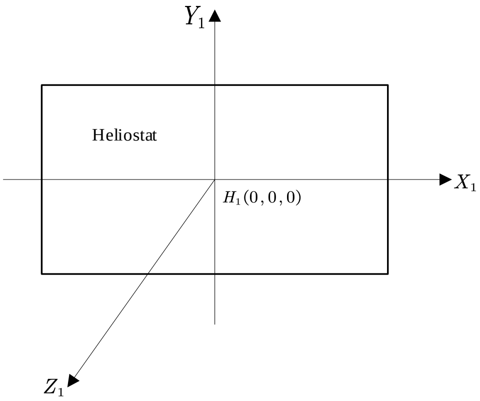

Figure 2 Mirror coordinate system

As Figure 2 above establishes the mirror coordinate system, the unit matrix of the transformation relation from the mirror coordinate system to the mirror field coordinate system is:

$$T=\begin{pmatrix} l_x & l_y & l_z \\ m_x & m_y & m_z \\ n_x & n_y & n_z \end{pmatrix} \quad (1)$$

(l_x, m_x, n_x),(l_y, m_y, n_y) ,(l_z, m_z, n_z) are the vector representations of the three axes of the mirror coordinate system in the mirror field coordinate system.

If the vector of the light ray in the mirror coordinate system is denoted as $\overrightarrow{L_H}$, and in the mirror field coordinate system as $\overrightarrow{L_0}$, then the transformation relation is as follows:

$$\overrightarrow{L_0} = \begin{pmatrix} l_x & l_y & l_z \\ m_x & m_y & m_z \\ n_x & n_y & n_z \end{pmatrix} \cdot \overrightarrow{L_H} \tag{2}$$

3） Establishment of the light-cone coordinate system

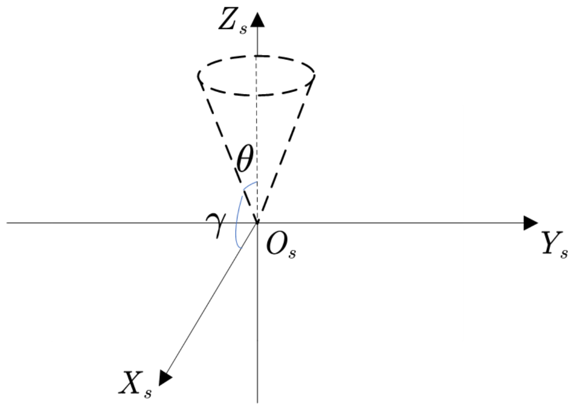

Figure 3 Light Cone Coordinate System

The diameter of the sun is much larger than the earth, the human eye to see the sun is a disk, so the sun's rays are not parallel rays, but there is a certain cone angle of conical rays[7], and its half-angle of the width of the spread of 4.65mrad, and therefore the establishment of the model needs to be established before the establishment of the light cone coordinate system as shown in Figure 3 above, the Y_s axis is perpendicular to the X_s axis and Z_s axis, the X_s axis is parallel to the ground, the cone that is the cone of the light in the figure, the Z_s axis is along the main line of the cone of light direction. The angle between the light ray in the light cone and the main ray is θ, and the angle between the light ray and the X_s axis is γ, then the vector expression of the light ray in the light cone coordinate system is:

$$\vec{s} = (\sin\theta\cos\gamma, \sin\theta\sin\gamma, \cos\theta) \tag{3}$$

Among others, $0 < \theta \leqslant 2.325 mrad$, $89997.675 mrad \leqslant \gamma \leqslant 90002.325 mrad$.

The conversion of the light-cone coordinate system and the mirror-field coordinate system is the same as that of the mirror coordinate system and the mirror-field coordinate system, and will not be repeated here.

2.1.2 Optical efficiency of the heliostat field

In this paper, the annual average optical efficiency is used to express the optical efficiency of the mirror field. Optical efficiency includes various sub-efficiencies such as shadow shading efficiency, cosine efficiency, atmospheric transmittance, collector truncation efficiency, specular reflectivity, etc. The terms related to each sub-efficiency are defined as follows:

♦ Shadow blocking loss: The shadow blocking loss includes the following parts: (1) The height of the absorption tower is not negligible, so the shadow generated by the absorption tower under the sun's irradiation will have a certain degree of blocking to the sun-stabilized mirrors. (2) The fixed-sun mirror is limited by the installation height and neighboring position, the sunlight may not be able to irradiate to the fixed-sun mirror which is arranged in the north, and after reflection, the light may be blocked by the fixed-sun mirror which is arranged in the south, and can not be irradiated to the collector, which results in the shadow shading loss.

♦Cosine Loss: The sunlight is tapered and limited by the accuracy of sun tracking by heliostat, it is difficult to keep the incident direction of sunlight parallel to the normal direction of heliostat, which causes the loss of energy reception by heliostat.

♦Atmospheric attenuation loss: The air contains dust, particles and other impurities that cause a certain amount of attenuation of the sun's rays during their propagation.

♦Collector truncation loss: Since the sun's rays are conical rays, they are also conical rays after being reflected by the heliostat, and the dispersion of the rays may result in the spot not being able to be fully irradiated on the collector, which results in truncation loss.

♦Mirror Reflectivity: The combined efficiency of the mirror reflectivity and the mirror in the case of a dirty mirror.

2.2. Modeling and solving

Figure 4 below establishes the heliostat reflection model, and calculates the annual average optical efficiency and annual average output thermal power of the heliostat field, as well as the annual average output thermal power per unit mirror area, with the following calculation steps.

STEP 1: Calculate the vector representation of the main ray in the mirror field coordinate system

First calculate the solar altitude angle [8] α_s:

$$\sin\alpha_s = \cos\delta\cos\varphi\cos\omega + \sin\delta\sin\varphi \tag{4}$$

where γ_s is the solar azimuth [8]:

$$\cos\gamma_s = \frac{\sin\delta - \sin\alpha_s\sin\varphi}{\cos\alpha_s\cos\varphi} \tag{5}$$

φ is the local latitude and ω is the solar time angle:

$$\omega = \frac{\pi}{12}(ST - 12) \tag{6}$$

ST is the local time, and δ is the angle of solar declination [9]:

$$\sin\delta = \sin\frac{2\pi D}{365}\sin\left(\frac{2\pi}{360}23.45\right) \tag{7}$$

D It is the number of days that start counting from the vernal equinox as the 0th day.

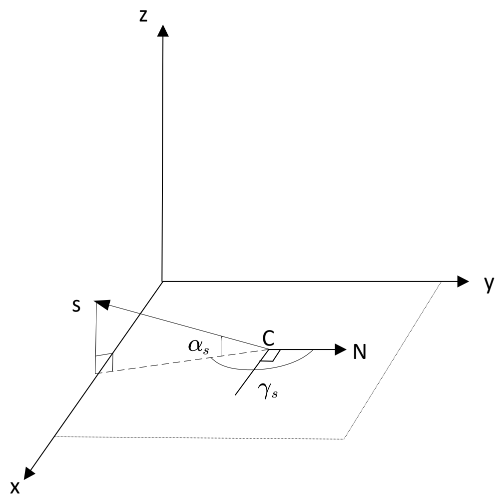

Figure 4 Reflection model of a heliostat

So the main ray vector is $\vec{m}$ $(\sin\gamma_s, \cos\gamma_s, \tan\alpha_s)$.

STEP 2: Solve the equations normal to a fixed heliograph

After the parameters related to the sun's altitude and azimuth angles are derived, the vectorial representation of the main sunlight rays in the mirror field coordinate system can be obtained: $\vec{m}$ $(\sin\gamma_s, \cos\gamma_s, \tan\alpha_s)$.

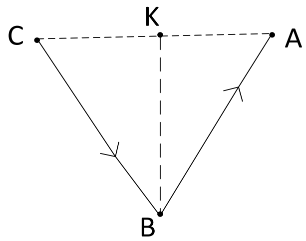

Figure 5 Incident and reflected light from the sun

Figure 5 shows the incident light from the sun and the reflected light of the incoming and outgoing relationship: point B is the main ray of sunlight incident point, point A is located on the collector, A on the normal BK symmetry point for C, CB is the main ray of sunlight, BA is the main ray of the reflected ray, so set $A(0,\ 0,\ z_1)$, $B(x_0,\ y_0,\ z_0)$, $C(x_2,\ y_2,\ z_2)$, $K(x_3,\ y_3,\ z_3)$, the vector representation of the main ray of light has been obtained before, so the linear equation of the incident line of light can be obtained:

$$\frac{x-x_0}{\sin\gamma_s}=\frac{y-y_0}{\cos\gamma_s}=\frac{z-z_0}{\tan\alpha_s} \tag{8}$$

Substituting the coordinates of point C into the equation of the line, and using x_2 for y_2 and z_2 , the coordinates of point C can be obtained:

$$C\ (x_2, \frac{x_2-x_0}{\tan\gamma_s}+y_0, \frac{\tan\alpha_s}{\sin\gamma_s}(x_2-x_0)+z_0) \tag{9}$$

By CB=AB

$$\sqrt{{x_0}^2+{y_0}^2+(z_0-z_1)^2}=|x_2-x_0|\sqrt{1+\left(\frac{1}{\tan\gamma_s}\right)^2+\left(\frac{\tan\alpha_s}{\sin\gamma_s}\right)^2} \tag{10}$$

The above equation gives two x_2:

$$x_{21}=\sqrt{\frac{{x_0}^2+{y_0}^2+(z_0-z_1)^2}{1+\left(\frac{1}{\tan\gamma_s}\right)^2+\left(\frac{\tan\alpha_s}{\sin\gamma_s}\right)^2}}+x_0 \tag{11}$$

$$x_{22}=x_0-\sqrt{\frac{{x_0}^2+{y_0}^2+(z_0-z_1)^2}{1+\left(\frac{1}{\tan\gamma_s}\right)^2+\left(\frac{\tan\alpha_s}{\sin\gamma_s}\right)^2}} \tag{12}$$

Consider that point C must be higher than point B, i.e., $z_2>z_0$, so add the following constraints to choose the correct x_2:

$$\frac{\tan\alpha_s}{\sin\gamma_s}(x_2-x_0)>0 \tag{13}$$

Find x_2 and then bring it back into the equation of the line to get the coordinates of point C. Since point K is the center point of AC, add the coordinates of the two AC points and divide by 2 to get the coordinates of point K. Take x_3 as an example:

$$x_3 = \frac{1}{2}(x_2 + 0) \tag{14}$$

The vector representation of the normal BK can then be obtained: $\left(\frac{x_2}{2} - x_0, \frac{y_2}{2} - y_0, \frac{z_2 - z_1}{2} - z_0\right)$.

STEP 3: Solve the unit matrix of the transformation relation from the mirror coordinate system and the light cone coordinate system to the mirror field coordinate system respectively

In the second step, the vector representation of the normal BK has been obtained, i.e., the vector representation of the z_1 axis in the mirror coordinate system in the mirror field coordinate system, so this study utilizes the relationship that the coordinate axes are perpendicular to each other, as well as the x-axis is parallel to the ground, and use the parameter in the BK vector to express the vector representations of the x_1 and y_1 axes in the mirror coordinate system in the mirror field coordinate system in the following process:

In order to facilitate the solution, so that $a_1 = \frac{x_2}{2} - x_0$, $b_1 = \frac{y_2}{2} - y_0$, $c_1 = \frac{z_2 - z_1}{2} - z_0$, that is, $\vec{z_1}(a_1, b_1, c_1)$, due to x_1 axis parallel to the ground, so set $\vec{x_1}(a_2, b_2, 0)$, $\vec{y_1}(a_3, b_3, c_3)$, by the two coordinate axes perpendicular to each other to calculate the relationship between $\vec{x_1}\left(a_2, -\frac{a_1}{b_1}a_2, 0\right)$, $\vec{y_1}\left(a_3, -\frac{a_2 a_3}{b_2}, \frac{b_1 a_2 a_3 - b_2 a_1 a_3}{b_2 c_1}\right)$, so that a_2, a_3 is equal to 1, then $\vec{x_1}\left(1, -\frac{a_1}{b_1}, 0\right)$, $\vec{y_1}\left(1, -\frac{1}{b_2}, \frac{b_1 - b_2 a_1}{b_2 c_1}\right)$, will be the vectors will be substituting into the transformation relationship matrix to get:

$$T = \begin{pmatrix} 1 & 1 & a_1 \\ -\frac{a_1}{b_1} & -\frac{1}{b_2} & b_1 \\ 0 & \frac{b_1 - b_2 a_1}{b_2 c_1} & c_1 \end{pmatrix} \tag{15}$$

Normalization yields the final unit matrix of conversion relations T .

The vector representation of the z_s axis in the light-cone coordinate system in the mirror-field coordinate system is obtained from $\vec{m}$ in the previous section. Since the unit matrix of the transformation relationship between the mirror coordinate system and the light-cone coordinate system to the mirror-field coordinate system is solved in the same way, the final matrix of the transformation relationship is given here directly:

$$T = \begin{pmatrix} 1 & 1 & \sin\gamma_s \\ -\tan\gamma_s & \frac{1}{\tan\gamma_s} & \cos\gamma_s \\ 0 & \frac{\cos\gamma_s + \tan\gamma_s \sin\gamma_s}{-\tan\gamma_s \tan\alpha_s} & \tan\alpha_s \end{pmatrix} \tag{16}$$

Normalization yields the final unit matrix of conversion relations T' .

STEP 4: Modeling shadow light blocking efficiency

Calculate the efficiency of shadow shading first to calculate the loss of shadow shading, that is, the calculation of x mirror at any point in the sun's rays of incident light or reflected rays of the reverse extension of the line whether to fall into the y mirror, and calculate the value of the mirror coordinates in the y mirror. Set a point in the x-mirror for $P_{H_1}(x_1, y_1)$, after the light falls into the y-mirror for $P_{H_2}(x_2, y_2)$, in order to find the latter's coordinates, then first of all to find out P_{H_1} in the mirror coordinate system in the coordinates of P'_{H_1} ; Secondly, to find out P'_{H_1} in the y-mirror surface coordinate system in the coordinates of P''_{H_1} ; Then the mirror field coordinate system in the light is converted to y-mirror surface coordinate system, and to find out that the intersection of the light and the y-mirror; Finally, determine whether P_{H_2} is in the mirror. The calculation process is as follows:

P_{H_1} Coordinates in the mirror field coordinate system P'_{H_1} :

$$P'_{H_1} = \begin{pmatrix} l_x & l_y & l_z \\ m_x & m_y & m_z \\ n_x & n_y & n_z \end{pmatrix} \cdot P_{H_1} + O_x = \begin{pmatrix} x'_1 \\ y'_1 \\ z'_1 \end{pmatrix} \tag{17}$$

O_x are the coordinates of the origin of the x-mirror coordinate system in the mirror field coordinate system$(x,\ y,\ z)$.

P'_{H_1} coordinates in the y-mirror coordinate system P''_{H_1} :

$$P''_{H_1} = \begin{pmatrix} l_x & l_y & l_z \\ m_x & m_y & m_z \\ n_x & n_y & n_z \end{pmatrix}^T \cdot \left(P'_{H_1} - O_y\right) = \begin{pmatrix} x_1'' \\ y_1'' \\ z_1'' \end{pmatrix} \tag{18}$$

O_x are the coordinates of the origin of the y-mirror coordinate system in the mirror field coordinate system$(x',\ y',\ z')$.

Converts light rays in the mirror field coordinate system to the y mirror coordinate system:

$$\overrightarrow{L_H} = \begin{pmatrix} l_x & l_y & l_z \\ m_x & m_y & m_z \\ n_x & n_y & n_z \end{pmatrix}^T \cdot \overrightarrow{L_0} = (m,\ n,\ k) \tag{19}$$

Use the coordinates and vectors obtained above to find $P_{H_2}(x_2,\ y_2,\ 0)$:

$$\text{leave it (to sb)} \ \frac{x_2 - x_1''}{m} = \frac{y_2 - y_1''}{n} = \frac{-z_1''}{k} \tag{20}$$

$$\text{catch (a disease)} \begin{cases} x_2 = \dfrac{kx_1'' - mz_1''}{k} \\ y_2 = \dfrac{ky_1'' - nz_1''}{k} \end{cases} \tag{21}$$

Then determine if P_{H_2} falls within the mirror range.

Using the traversal algorithm, take a step size of 0.6, take 100 points uniformly on each mirror to study them separately, determine whether the incident or reflected ray of the sun's rays at the point where they are located is the reverse extension of the sun's rays falling into the nearest mirror where it is to the north or to the south, and finally use the following formula to calculate the shadow shading efficiency η_{sb} :

$$\text{Loss of shadow masking} = \frac{\text{Total number of points that will fall into other mirrors}}{\text{Total number of points taken}} \tag{22}$$

$$\eta_{\text{sb}} = 1 - \text{Loss of shadow masking} \tag{23}$$

STEP 5: Modeling Truncation Efficiency

The sun ray is a bunch of conical rays, in order to solve the collector truncation efficiency, this paper adopts the ray tracing method, as shown in figure 6 for a number of rays in a bunch of light cone in the direction of the half-angle spreading width with a uniform step to divide, and calculate the coordinates of the falling point of multiple rays reflected to the collector by the heliostat.

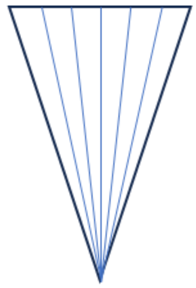

Figure 6 Uniform division of a beam of light cone into a number of rays

The procedure for calculating the coordinates of the drop point is as follows:

P_{H_1} Coordinates in the mirror field coordinate system P'_{H_1}:

$$P'_{H_1} = T \cdot P_{H_1} + O_x = \begin{pmatrix} x'_1 \\ y'_1 \\ z'_1 \end{pmatrix} \tag{24}$$

Set a light in the light cone for $\overrightarrow{L_s} = (a, b, c)$, because the light path can be reversed, and the light cone coordinate system to the main light for z_s axis, so the incident light after reflection of the reflected light is still in the light cone, that is, $\overrightarrow{L_s} = (a, b, c)$ can also be expressed as a reflected light, which will be transformed into the mirror field coordinate system:

$$\overrightarrow{L_{sg}} = T' \cdot \overrightarrow{L_s} = (a_1, b_1, c_1) \tag{25}$$

See STEP3 for specific calculations for T and T' above.

♦ Find the equation of the reflected ray:

$$\frac{x - x_1}{a_1} = \frac{y - y_1}{b_1} = \frac{z}{c_1} \tag{26}$$

♦ At $z \in [76, 84]$, determine whether the reflected light satisfies the following inequality:

$$x^2 + y^2 < r^2 \tag{27}$$

If satisfied then this reflected light can be captured by the collector.

♦ Using an ergodic algorithm, 20 rays are taken for each light cone in STEP4 after removing the shadow blocking part of the rays, and their reflected rays are calculated separately to see whether they can be captured by the collector or not, and then the truncation efficiency is calculated according to the following equation:

$$\eta_{\text{trunc}} = \frac{\text{Total number of light received by the collector}}{\text{Total number of specularly fully reflected rays} - \text{Total light lost to shadow blockage}} \tag{28}$$

STEP 6: Solving for cosine efficiency

Assuming an angle of incidence of σ, the cosine efficiency is:

$$\begin{cases} \eta_{\cos} = \cos\ \sigma \\ \cos\ \sigma = \dfrac{\vec{m} \cdot \overrightarrow{KB}}{|\vec{m}|\,|\overrightarrow{KB}|} \end{cases} \tag{29}$$

Where $\vec{m}$ is the solar ray vector and $\overrightarrow{KB}$ is the heliograph normal vector.

STEP 7: Solving for atmospheric transmittance

The formula for atmospheric transmittance[10] is given below:

$$\eta_{\mathrm{at}} = 0.99321 - 0.0001176 d_{\mathrm{HR}} + 1.97 \times 10^{-8} \times d_{\mathrm{HR}}^2 \quad (d_{\mathrm{HR}} \leq 1000) \tag{30}$$

Where, d_{HR} indicates the distance from the center of the mirror to the center of the collector (unit: m).

$$d_{HR} = \sqrt{x_0^2 + y_0^2 + (z_0 - 80)^2} \tag{31}$$

STEP 8: Calculation of heliostat optical efficiency

The optical efficiency can be found by taking the specular reflectance η_{ref} as a constant of 0.92:

$$\eta = \eta_{\mathrm{sb}} \eta_{\cos} \eta_{\mathrm{at}} \eta_{\mathrm{trunc}} \eta_{\mathrm{ref}} \tag{32}$$

The annual average optical efficiency is obtained by summing and averaging the optical efficiencies calculated for the 12 months of the year.

STEP 9: Calculation of annual average thermal power

The output thermal power of the heliostat field E_{field} is

$$E_{\mathrm{field}} = \mathrm{DNI} \cdot \sum_{N}^{i} A_i \eta_i \tag{33}$$

Where η_i is the optical efficiency of the ith mirror, which can be found from the above steps; A_i is the light-gathering area of the ith mirror; N is the total number of fixed-sun mirrors; and DNI is the normal direct radiation irradiance[11]:

$$\mathrm{DNI} = G_0 \left[a + b \exp\left(- \frac{c}{\sin \alpha_s} \right) \right] \tag{34}$$

$$a = 0.4237 - 0.00821(6 - H)^2 \tag{35}$$

$$b = 0.5055 + 0.00595(6.5 - H)^2 \tag{36}$$

$$c = 0.2711 + 0.01858(2.5 - H)^2 \tag{37}$$

Where, G_0 is the solar constant, the value is 1.336kW/m ;$^2 H$ is the altitude, in this paper the altitude is taken as 3km, α_s is the solar altitude angle, which can be solved in STEP1. The annual average thermal power output is obtained by summing and averaging the output thermal power calculated for 12 months of the year.

STEP 10: Calculate Average annual thermal power per unit mirror area

The average annual thermal power per unit mirror area is obtained by dividing the average annual thermal power output obtained in STEP9 by the total mirror area of the fixed-sun mirror.

3. Results presentation

In this paper, a case simulation of a heliostat mirror field in a circular area with coordinates of Gansu region (98.5°E, 39.4°N), an altitude of 3000 meters and a radius of 350 meters is performed, and the data are obtained from http://www.mcm.edu.cn/. The mirror field coordinate system was established with the center of the circle as the origin, due east direction as the x-axis positive, due north direction as the y-axis positive, and vertical ground upward as the z-axis positive. Among them, the absorption tower is 80 m high, the collector is 8 m high, 7 m diameter cylinder, the height of the collector center to the ground is the height of the absorption tower; the fixed-sun mirror mirror is 6 m×6 m, and the installation height is at 4 m. Through the above steps for the annual average optical efficiency, annual average output thermal power, and the unit mirror area annual average output thermal power is calculated, and the Table 1 shows the average optical efficiency and output power per month. Table 1 shows the average optical efficiency and output power per month, and Table 2 shows the average optical efficiency and output power per year:

Table 1 Average optical efficiency and output power on the 21st day of each month

Dates	Average optical efficiency	Average cosine efficiency	Average shadow masking efficiency	Average truncation efficiency	Average thermal power output per unit area of mirror (kW/m2)
January 21	0.5331	0.6867	0.9098	0.9317	0.2548
February 21	0.5331	0.7040	0.9105	0.9010	0.2547
March 21	0.5346	0.7286	0.9167	0.8605	0.2554
April 21	0.5448	0.7454	0.9169	0.8594	0.2603
May 21	0.5531	0.7552	0.9192	0.8611	0.2643
June 21	0.5589	0.7583	0.9210	0.8657	0.2671
July 21	0.5536	0.7557	0.9194	0.8613	0.2645
August 21	0.5461	0.7465	0.9168	0.8606	0.2609
September 21	0.5352	0.7302	0.9161	0.8604	0.2557
October 21	0.5342	0.7093	0.9139	0.8894	0.2553
November 21	0.5346	0.6902	0.9103	0.9273	0.2555
December 21	0.5279	0.6811	0.9063	0.9383	0.2522

Table 2 Annual average optical efficiency and output power table

Average annual optical efficiency	Average annual cosine efficiency	Average annual shadow shading efficiency	Average annual truncation efficiency	Average annual thermal power output (MW)	Average annual thermal power output per unit area of mirror (kW/m^2)
0.5408	0.7243	0.9147	0.8847	16.2327	0.2584

From tables 1 and 2, it can be concluded that the results of Monte Carlo simulation of the trajectory of the light rays give some indication of the annual average optical efficiency and annual average thermal power of the site, which are approximate to the annual average optical efficiency and annual average thermal power data given for the site by the Higher Education Cup. The shading of the fixed heliostat field by the absorption tower in this case is calculated to be so small as to be almost negligible. The reason for the higher annual average truncation efficiency versus during the winter months is that the sun's altitude angle is small enough that most of the sunlight is not reflected and then interfered with by the other heliostats, and is able to reach the absorber tower without any problems. Causes the data to show that the site's fixed-sun mirror energy supply is more average and stable from month to month. Based on the fact that the low annual average cosine efficiency is the most important obstacle affecting the reception of optical energy at this site, adjusting the angle between the heliostat and the ground is the most effective way to increase the annual average optical efficiency and annual average thermal power at this site.

4. Conclusions

This study simulates the relaying process of light rays in mirrors by using coordinate transformation and Monte Carlo simulation, construct a suitable mathematical model, and solve the annual average optical efficiency, annual average output thermal power, and annual average output thermal power per unit of cross-sectional area of the heliostat mirror field. Firstly, the normal equation of each heliostat is obtained by using the solar altitude angle and azimuth angle, and the mirror coordinate system is established to study the reflection of the light, and the corresponding shadow blocking efficiency is calculated; then the light cone coordinate system is established to simulate the dispersion of light cone rays on the reflected rays, so as to calculate the truncation efficiency; then the cosine efficiency is calculated by the incidence angle, and the annual average optical efficiency, annual average output thermal power and unit average output thermal power of cross-section area are obtained by the relevant formulas in the end. The annual average optical efficiency, the annual average output thermal power and the annual average output thermal power per unit of cross-sectional area are finally obtained by the relevant formulae.

In this paper, due to the transformation of the mirror coordinate system, light cone coordinate system and mirror field coordinate system, there are many parameters, and the model is also more complicated, and the calculation is huge. Therefore, in the subsequent research, it is necessary to further review the relevant literature to seek ways to simplify the calculation of shadow shading loss and collector truncation loss. At the same time, this paper only simulates and calculates the relevant indexes of the heliostat mirror field, and does not propose the optimal configuration method of the heliostat mirror field, so further research is needed on how to select typical heliostat mirror field data and adopt suitable mathematical models.

References

[1] Lei Xiandao, Shuai Qifeng, Zhang Zhuoqun, Zhang Zhengxiang. The principle of tower solar thermal power generation system [J]. Hydropower and New Energy, 2023, 37(12): 10-13.

[2] Huang Ju, Yan Zhiguo, Deng Biao et al. Current status of research on mirror field design software for tower solar thermal power plants [J]. Oriental Electric Review, 2023, 37(02): 41-47.

[3] Lv Caixia. Influence of heliostat parameters on the performance of tower-type solar concentrating collector system [J]. Energy Conservation, 2023, 42(05): 34-37.

[4] Liu Jianxing. Modeling simulation of optical efficiency and optimal arrangement of heliostat mirror field for tower-type photovoltaic power plant [D]. Lanzhou Jiaotong University, 2022.

[5] Gao Bo, Sun Hao, Liu Sheng. Optimized arrangement of mirror field for solar thermal power plant based on improved whale algorithm [J]. Journal of Solar Energy, 2023, 44(10): 209-217.

[6] Ding Q, Zeng ZY, Chen WZ et al. A method for evaluating the effective mirror area of a fixed-sun mirror field [J]. Journal of Solar Energy, 2021, 42(09): 184-189.

[7] P. Zhang, Z.S. Xi, W.H. Hua et al. Calculation method of optical efficiency of solar tower photothermal mirror field [J]. Technology and Market, 2021, 28(06): 5-8.

[8] HUANG Yan, MAO Zhonghua, YU Jian et al. Design of intelligent follower solar light tower [J]. Science and Technology Innovation, 2024(06): 225-228.

[9] Z. J. Cai, Solar shadow localization [J], Mathematical modeling and its applications, 2015, 4(4): 25-33.

[10] O. Farges, J.J. Bezian, M. El Hafi, Global optimization of solar power tower systems using a Monte Carlo algorithm: application to a redesign of the PS10 solar thermal power plant [J], Renewable Energy, 2018, 119: 345-353.

[11] Du Yuhang et al, Analysis of the effects of different focusing strategies of heliostats in tower-type photovoltaic power plants [J], Journal of Power Engineering, 2020, 40(5): 426-432.